



Konrad Dadej\*, Barbara Surowska

Lublin University of Technology, Faculty of Mechanical Engineering, Department of Materials Engineering, ul. Nadbystrzycka 36, 20-618 Lublin, Poland

\*Corresponding author. E-mail: k.dadej@pollub.pl

Received (Otrzymano) 01.06.2016

## ANALYSIS OF COHESIVE ZONE MODEL PARAMETERS ON RESPONSE OF GLASS-EPOXY COMPOSITE IN MODE II INTERLAMINAR FRACTURE TOUGHNESS TEST

The purpose of the performed study was to provide the best possible representation of the response of a beam subjected to Interlaminar Fracture Toughness testing in Mode II in the course of the End Notched Flexure test. The beam was modelled numerically with the results obtained in experimental tests. Furthermore, analysis was carried out in order to determine the parameters of the traction-separation law in the ABAQUS program defined for the cohesion layer, which have a key impact on the response of the cracking composite beam in the End Notched Flexure test. Experimental tests were conducted on composite beams reinforced with 'E' type fibre glass in an epoxy resin matrix. A composite plate 4.3 mm thick produced in the autoclave process was cut into beams with dimensions of 150 x 25 mm in a manner ensuring an initial delamination length of 30 mm. A numerical model of the composite material with a cohesion layer based on the determined value of fracture energy in Mode II was developed in the ABAQUS program on the basis of experimental tests. The analysis of the impact of the parameters defined in the traction-separation law on the response of the cracking composite beam was conducted on the basis of numerical simulations. The results obtained from the numerical analyses show a strong dependence between the cohesion layer parameters and the response of the composite beam, also in case of a constant value of fracture toughness. It was determined which of the parameters defined in the ABAQUS program have a key impact on the composite cracking process. Finally, very good convergence was achieved for the beam response in the numerical model and in the experiment in terms of force-displacement curves, the critical value of force and displacement causing energy release and crack length in the composite.

**Keywords:** interlaminar fracture toughness, mode II, cohesive zone method, numerical modelling

## ANALIZA PARAMETRÓW MODELU WARSTWY KOHEZYJNEJ NA ODPOWIEDŹ KOMPOZYTU EPOKSYDOWO-SZKLANEGO W TESTACH WYTRZYMAŁOŚCI MIĘDZYWARSTWOWEJ W II SPOSOBIE PĘKANIA

Celem przeprowadzonych prac było jak najlepsze odwzorowanie odpowiedzi belki poddanej badaniu Interlaminar Fracture Toughness w Mode II w teście End Notched Flexure, zamodelowanej numerycznie z wynikami otrzymanymi w testach doświadczalnych. Ponadto, przeprowadzona została analiza mająca na celu zbadanie, które z parametrów prawa trawienia - separacja w programie ABAQUS definiowanego dla warstwy kohezyjnej mają kluczowy wpływ na odpowiedź pękającej belki kompozytowej w badaniu End Notched Flexure. Przedmiotem badań eksperymentalnych były belki kompozytowe wzmocnione włóknem szklanym typu E w osnowie żywicy epoksydowej. Płytę kompozytową o grubości 4,3 mm wytworzoną metodą autoklawową pocięto na belki o wymiarach 150 x 25 mm w taki sposób, żeby otrzymać długość początkową delaminacji równą 30 mm. W programie ABAQUS na podstawie badań eksperymentalnych został opracowany model numeryczny materiału kompozytowego wraz z warstwą kohezyjną bazującą na wyznaczonej wartości energii pęknięcia w Mode II. Na podstawie symulacji numerycznych przeprowadzono analizę wpływu parametrów definiowanych w prawie trawienia - separacja na odpowiedź pękającej belki kompozytowej. Wyniki analiz numerycznych wskazują na dużą zależność pomiędzy wartościami parametrów warstwy kohezyjnej a odpowiedzią belki kompozytowej również przy stałej wartości energii pęknięcia. Przedstawiono, które z parametrów definiowanych w programie ABAQUS mają kluczowy wpływ na proces pęknięcia kompozytów. Finalnie, osiągnięta została bardzo duża zbieżność odpowiedzi belki w modelu numerycznym i eksperymencie, biorąc pod uwagę charakterystyki siła-przemieszczenie, wartość krytyczną siły i przemieszczenia powodujących uwolnienie energii i wzrost pęknięcia w kompozycie.

**Słowa kluczowe:** wytrzymałość na pęknięcie, II sposób pęknięcia, metoda warstwy kohezyjnej, modelowanie numeryczne

## INTRODUCTION

Polymer composite fibrous materials is a group of modern equipment, e.g. wind turbines, aerospace and materials finding increasingly more applications in the automotive industry. In comparison to conventional

materials (e.g. metal and ceramic materials), composite materials are characterized by the occurrence of additional forms of damage, i.e. delamination, the most frequently occurring between layers of fibres with different orientation [1, 2]. Intra-laminar cracks are another type of composite damage occurring in the form of polymer matrix cracks oriented in accordance with the fibre orientation direction without disturbing their continuity. These forms of damage deteriorate laminate stiffness and significantly increase the risk of damage in the case of the structure subjected to further work, though they do not deteriorate the tensile strength significantly. Therefore numerous experimental tests and numerical simulations are carried out in order to ensure adequate modelling of intra-laminar cracks and delaminations in composite materials exposed to damage in the course of operation [3]. The Finite Element Method (FEM) is used in this case to assess the extent of damage in loaded structures and to forecast residual strength [4-6]. ABAQUS and ANSYS are commercially available programs the most frequently described in literature which are dedicated for numerical computations by means of the Finite Element Method. In the case of major damage forms of fibrous composites e.g. matrix or fibre cracking caused by tensile or compressive loads, the ABAQUS built-in functions are usually sufficient to accurately predict this type of damage. However, in the case of intra-laminar cracks or delaminations, investigators use additional techniques enabling material separation in order to simulate cracking, e.g. the Cohesive Zone Method (CZM) or the Virtual Crack Closure Technique (VCCT) because built-in modules are insufficient. In the scope of composite materials, CZM is regarded as the most convenient technique used for crack modelling. An important advantage of CZM consists in adequate representation of the global response of cracking material and in its relatively simple definition. Moreover, in comparison to VCCT, the CZM technique makes it possible to forecast not only crack propagation but also its initiation [7].

Dugdale [8] and Barenblatt [9] proposed the material cohesion theory which has been used to define the traction-separation ( $t$ - $s$ ) law, i.e. the relationship between traction-stress in the interface ( $t_{ss}$ ), and displacement jump ( $\delta$ ) between two parts of material being separated. In later works, traction-separation ( $t$ - $s$ ) law has been used to describe cracking in a discrete manner, in the places of the material where crack growth is predicted. According to ( $t$ - $s$ ) theory, crack initiation and growth are associated with energy dissipation in the material and are irreversible. There are various shapes of constitutive models in ( $t$ - $s$ ) law. Camanho et al. [10] as well as Turon et al. [11] proposed a bilinear cohesive traction-separation law which has been implemented into the ABAQUS environment. In ABAQUS,  $t$ - $s$  law defines an elastic range of interface where it is possible to load and unload the material without causing any damage. The critical point which corresponds to the start of damage and limit amount of energy to be sup-

plied to the structure in order to cause complete material separation are also defined. The initial elastic range is determined by means of stiffness parameter ( $K$ ). The linear response of the interface is observed till achievement of the  $t$  point resulting in material weakening (degradation of cohesive elements) and crack growth thereafter. Thorough analysis representing cohesive elements being loaded and the corresponding points within  $t$ - $s$  law ranges has been presented in the study published by Shor and Vaziri [12]. In the ABAQUS program, it is possible to define  $t$ - $s$  law for three Fracture Modes (I, II and III) introducing three values of Critical Strain Energy Release Rate (SERR)  $G_{Ic}$ ,  $G_{IIc}$ ,  $G_{IIIc}$ , Interface Stiffness  $K_{nn}$ ,  $K_{ss}$ ,  $K_{tt}$ , and traction stress  $t_{nm}$ ,  $t_{ss}$ ,  $t_{tt}$  correspondingly.

In recent years, there have been numerous studies relating to numerical analyses of composite material damage by means of CZM. Borg et al. [13] modelled DCB, ENF and MMB tests by means of the Cohesive Zone Method for conventional composites. Libin Zhao et.al. [14] applied the numerical model for forecasting the delamination propagation process in a CFRP composite loaded in Mode I and Mixed Mode I/II using cohesive elements. Lopes et al. [15] applied CZM in order to characterize the damage of a CFRP composite in the intra-laminar plane and to estimate the delamination surface area in a low-velocity impact test. Jing-Fen Chen [16] defined the numerical model based on CZM and used this model for the progressive failure analysis of an AS4/PEEK composite. Multiple delamination growth research was continued and modelled by means of bilinear  $t$ - $s$  law by Liu et al. [7].

However, regardless of the numerous applications of CZM, analyses of the impact of the defined parameters in the cohesive layer on the obtained response of loaded structures are still being continued. Rots [17], Volokh [18] and Chandra et al. [19] investigated the impact of the shape of a constitutive  $t$ - $s$  model on the obtained response of the cracking material. Additionally, despite many the advantages of CZM, the fact that it has still not been unified impedes its application. Therefore engineers and investigators simulating the cracking process have to define the parameters characterizing the mechanical behaviour of the cohesive layer according to their own experience. The process associated with proper selection of the  $K$  and  $t$  parameters is time consuming and unclear because these parameters do not have their equivalents in real material constants and are only the virtual values used to define the proper strength of the interface in a numerical model. Owing to the aforesaid problems, the present study encompasses analysis of the impact of individual parameters defined in CZM in the ABAQUS program on the response of a composite beam subjected to load in cracking Mode II. The purpose of the performed numerical analyses was to achieve the best possible representation of numerical  $P$ - $d$  response of the modelled ENF beam with the experimental tests results. Furthermore, analysis was performed in order to determine which parameters

in *t-s* law have the key impact on the response of the modelled ENF beam and to find the value ranges of these parameters which can be used in further, more complicated analyses.

## METHODOLOGY

### Material

Experimental tests were carried out on unidirectional GFRP composites based on E-glass fibres (GURIT SE 70, UK) with the thickness of a single layer of 0.255 mm. The specimens for tests consisted of composite layers and a teflon insert were characterized by the following dimensions: length 150 mm, width 24 mm, thickness 4 mm, thickness of the Teflon insert 20 μm. The research material was produced in the Department of Materials Engineering of the Lublin University of Technology in the autoclave process. The process parameters marked as ‘QUICK’ in the study published by Bienias et al. [20] were used to produce the research material.

### End Notched Flexure tests

The End Notched Flexure (ENF) [21] test was used in order to determine the Critical Strain Energy Release Rate ( $G_{IIc}$ ) in Mode II. The distance between the supports was equal to  $2L = 100$  mm, the radius of the lower supports  $r = 1.5$  mm, the radius of the upper indenter  $R = 3$  mm and the preliminary length of delamination  $a_0 = 30$  mm. The test was carried out at the velocity of 2 mm/min until the time of energy release - specimen cracking. The stand for the ENF tests is shown in Figure 1.

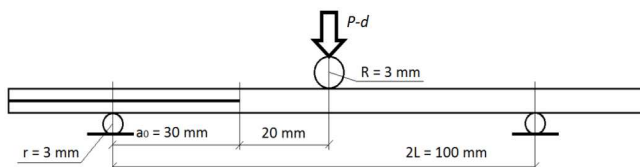


Fig. 1. Test conditions for composites testing by means of ENF method  
Rys. 1. Warunki testu do realizacji testów kompozytów metodą ENF

The force-deflection (*P-d*) curve was recorded during the ENF test. The SERR  $G_{IIc}$  values were calculated by means of equation (1) [22]:

$$G_{IIc} = \frac{9Pda_0^2}{2b(2L^3 + 3a_0^3)} \quad (1)$$

where  $G_{IIc}$  is the Critical Energy Release Rate in Mode II calculated by means of Beam Theory (BT),  $P$  is the critical force at the time of energy release,  $d$  is the central deflection of the composite beam at the time of critical force achievement,  $a_0$  is the length of the initial crack,  $b$  is the width of the specimen,  $L$  is the half distance between the lower loading points.

## Finite Element Analysis

Commercial ABAQUS/Standard software was used for numerical analyses of the End Notched Flexure Tests on the composite materials by the Finite Element Method. Figure 2 illustrates the discrete model of the specimen and the applied boundary conditions.

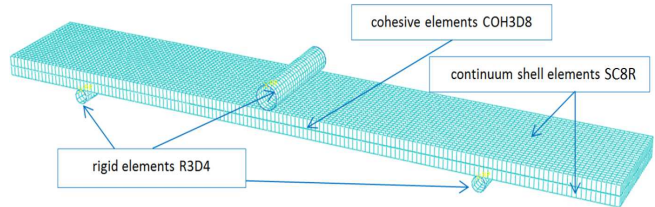


Fig. 2. Discrete 3D model and applied boundary conditions of modelled ENF test configuration

Rys. 2. Model dyskretny 3D oraz warunki brzegowe w modelowanym teście ENF

The two lower supports were fixed in all directions and the enforced displacement of the upper indenter was equal to 10 mm. The indenter response (force) to pushing it into the beam was recorded in the course of the test.

### Composite layer

The composite layers were modelled as elastic material by means of C3D8R elements (An 8-node linear brick, reduced integration, hourglass control). The built-in ‘lamina’ model was used to define the anisotropic composite material. The experimentally determined mechanical properties of the used composite material are marked ‘QUICK’ and presented in the experimental part of the present study.

### Cohesive Zone Model

In ABAQUS/Standard, the composite material crack zone was modelled using CZM by means of standard COH3D8 cohesive elements. The mesh density was equal to 1x1 mm and the thickness of the cohesive layer was equal to 0.05 mm. The parameters of the bilinear constitutive model of the traction-separation law which were used in this paper are presented in Figure 3.

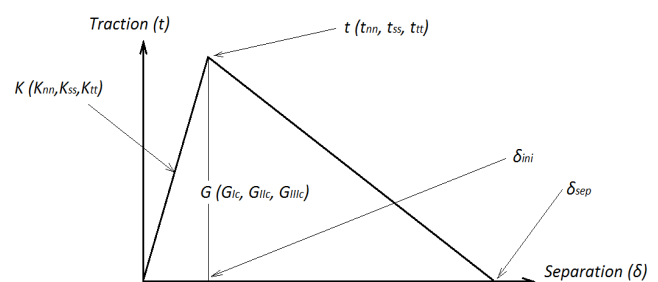


Fig. 3. Parameters of cohesive zone model in bilinear traction-separation law

Rys. 3. Parametry modelu warstwy kohezji w bilinearnej prawie trawcja-separacja

The parameters applied in  $t$ - $s$  law, i.e.  $K_{ss}$  and  $t_{ss}$ , in accordance with equation (2), determine the strain characterized by the initiation of cohesive damage  $\delta_{ini}$ . According to equation (3), simultaneously with the definition of cracking energy  $G_{IIc}$ , the value of strain  $\delta_{sep}$  is determined, which corresponds to complete separation of the connected surfaces.

$$\delta_{ini} = \frac{t_{ss}}{K_{ss}} \quad (2)$$

$$G_{IIc} = \frac{\delta_{ini} * t_{ss}}{2} + \frac{(\delta_{sep} - \delta_{ini}) * t_{ss}}{2} \quad (3)$$

### Interphase elastic behaviour

The mechanical behaviour of the cohesive layer in the elastic range is characterized by the following equation (4) [23]:

$$t = \begin{Bmatrix} t_{nn} \\ t_{ss} \\ t_{tt} \end{Bmatrix} = \begin{bmatrix} K_{nn} & K_{ns} & K_{nt} \\ K_{ns} & K_{ss} & K_{st} \\ K_{nt} & K_{st} & K_{tt} \end{bmatrix} \begin{Bmatrix} \delta_n \\ \delta_s \\ \delta_t \end{Bmatrix} = K \delta \quad (4)$$

where  $t$ ,  $t_{nn}$ ,  $t_{ss}$ ,  $t_{tt}$  are tractions in the cohesive,  $K$ ,  $K_{nn}$ ,  $K_{ss}$ ,  $K_{tt}$  are the cohesive layer stiffness,  $\delta$ ,  $\delta_n$ ,  $\delta_s$ ,  $\delta_t$  are the separation displacements of the cohesive; respectively in global, normal, shear and transverse directions.

### Interphase damage initiation

The Quadratic Stress Criterion (QUADS) available in ABAQUS has been applied in order to define the point associated the beginning of the cohesive element degradation process. The QUADS criterion is met when the following equation is met (5) [23]:

$$\left\{ \frac{t_{nn}^0}{t_n^0} \right\}^2 + \left\{ \frac{t_{ss}^0}{t_s^0} \right\}^2 + \left\{ \frac{t_{tt}^0}{t_t^0} \right\}^2 = 1 \quad (5)$$

where  $t_n^0$ ,  $t_s^0$  and  $t_t^0$  represent the peak values of the contact stress when the separation is either purely normal to the interface or purely shear or transverse direction, respectively; ' $\langle \rangle$ ' is a Macaulay bracket.

### Interphase damage evolution

In the cohesive layer, after the achievement of  $t_{ss}$ , growth of cohesive element stiffness degradation takes place. The progressing load increases the damage of the finite element (reduces its stiffness) and is followed by removal of the deformed finite element and finally by material separation. The cohesive element stiffness degradation is expressed by means of the following equation (6) [23]:

$$t_{ss} = (1 - D) \bar{t}_{ss} \quad (6)$$

where  $D$  is the damage variable, which starts from the value of 0 in undamaged cohesive elements. The value of  $D$  tends to 1 when cohesive damage occurs. The bigger the  $D$  coefficient is, then the effective  $t_s$  is

smaller and the mechanical response of the cohesive element is weaker.

## RESULTS AND DISCUSSION

### Experimental tests

Figure 4 illustrates the  $P$ - $d$  curves recorded in the experimental tests. Three experimental ENF tests were executed and used as the basis for calculating the SERR  $G_{IIc}$  values in accordance with equation (1).

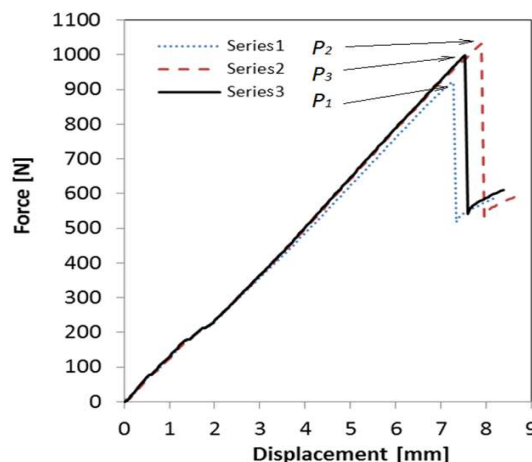


Fig. 4. Results of experimental interlaminar fracture toughness ENF test in Mode II

Rys. 4. Wyniki eksperymentalnych testów wytrzymałości międzywarstwowej ENF w II sposobie pękania

The  $P$ - $d$  curves can be conventionally subdivided into three parts. The first part illustrates the linear  $P$ - $d$  relationship between the beginning of the investigation ( $d = 0$  mm) and the point indicating energy release and crack propagation ( $P$ ). Energy release, a sudden reduction in force and unstable crack growth are observed in the second phase. A similar unstable growth of delaminations was observed by Budzik et al. [21] and is associated with a limited R-curve of the stable crack propagation state in general ENF type tests. The third phase occurring after the cracking process is also characterized by linearity. However, in order for initial crack  $a_0$  to extend to the length of  $a_1$ , beam compliance  $C$  ( $C = d/P$ ) was also increased and finally resulted in a different slope of the  $P$ - $d$  curve after an unstable crack.

TABLE 1. Results obtained from experimental ENF tests on GFRP material

TABELA 1. Wyniki otrzymane w testach doświadczalnych ENF na materiale GFRP

Sample no.	$d$	$P$	$G_{IIc}$
	[mm]	[N]	[N/mm]
1	7.27	921	3.41
2	7.89	1032	4.15
3	7.53	998	3.83
Average ( $\pm$ Student T-; $\alpha = 0.05$ )	7.56 ( $\pm 0.35$ )	984 ( $\pm 64$ )	3.80 ( $\pm 0.42$ )

## Bending stiffness

The impact of the elastic properties on composite beam stiffness with preliminary delamination (length of  $a_0$ ) was tested in order to perform analysis of the impact of the defined material properties on the response of the composite specimen subjected to ENF testing. The basic mechanical properties defined for the composite material in the ABAQUS program by means of a simple material model ('lamina') -  $E_1$ ,  $E_2$ ,  $\nu_{12}$ ,  $G_{12}$ ,  $G_{13}$ ,  $G_{23}$  were taken into account. Figure 5 illustrates the results obtained from numerical simulations of the cracking process in a GFRP composite in Mode II.

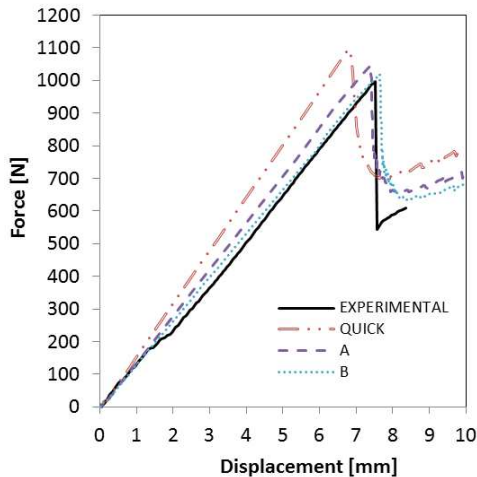


Fig. 5. Response of ENF specimen depending on assumed value of Young's modulus  $E_1$ ; marking: QUICK, A, B in accordance with Table 2

Rys. 5. Odpowiedź próbki w testach ENF w zależności od wartości modułu Younga  $E_1$ ; oznaczenia: QUICK, A, B według tabeli 2

According to Figure 5, the response of the ENF beam modelled by means of experimentally determined mechanical properties ('QUICK') is similar to the response recorded in the experimental tests but there is a difference in the slope in the linear range in the initial phase. In order to achieve the best possible conformity between the numerical model and the experiment, the mechanical properties of the modelled material were properly adapted. As a result of reducing the ABAQUS elastic input parameter - Young's modulus  $E_1$  (from 35400 to 28875 MPa), high conformity between the numerical model and the experiment was achieved in the first linear range of registered  $P-d$  characteristics. It was observed that the value of Young's modulus parallel to fibre direction  $E_1$  is the key factor for composite beam stiffness. Similar analyses of material model adaptation are also described in literature. The numerical model was adapted for experimental tests by Joki et.al. [24] by changing the cohesive layer parameters in Double Cantilever Beam (Mode I) tests. Table 2 contains the mechanical properties of the material which were changed in the numerical model.

Figure 6 illustrates the  $P-d$  curves obtained in the numerical simulations using various material properties (the mechanical properties were changed, except  $E_1$ ).

TABLE 2. Elastic mechanical properties of modelled composite material

TABELA 2. Sprężyste właściwości mechaniczne modelowanego materiału kompozytowego

Mechanical constant / test symbol:	QUICK	A	B	C	Unit
Young's modulus in 1-direction $E_1$	35400	30800	28875	28875	MPa
Young's modulus in 2-direction $E_2$	8200	8200	8200	6560	MPa
Poisson's ratio $\nu_{12}$	0.31	0.31	0.31	0.25	-
Shear modulus $G_{12}$	2100	2100	2100	1680	MPa
Shear modulus $G_{13}$	2100	2100	2100	1680	MPa
Shear modulus $G_{23}$	1750	1750	1750	1400	MPa

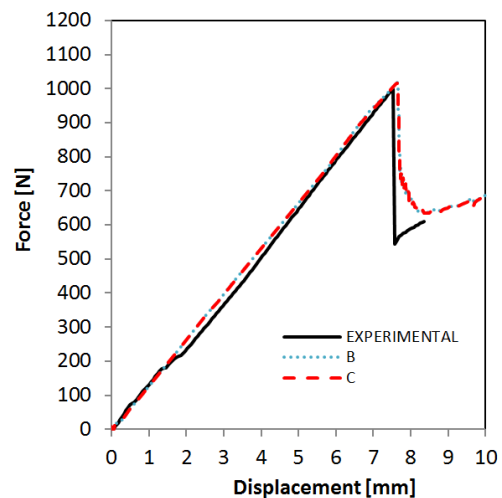


Fig. 6. Response of ENF GFRP specimen depending on remaining assumed mechanical properties of composite material; B, C marking in accordance with Table 2

Rys. 6. Odpowiedź próbki GFRP w testach ENF w zależności przyjętych pozostałych właściwości mechanicznych materiału kompozytowego; oznaczenia B, C według tabeli 2

It can be observed that the impact of Young's modulus  $E_2$  on beam response in the ENF test is negligible like the other defined elastic properties - Poisson's ratio  $\nu_{12}$ , as well as the values of shear stiffness moduli  $G_{12}$ ,  $G_{13}$ ,  $G_{23}$ . A similar effect was recorded by Soto et al. [25], who observed that in the case of a unidirectional carbon fibre composite, the specimen bending stiffness in Mode II mainly depends on the value of Young's modulus  $E_1$ .

## Cohesive Zone Model

In the second phase of the study, analysis of the influence of  $t-s$  law parameters ( $K_{ss}$ ,  $t_{ss}$ ,  $G_{IIc}$ ) in the cohesive layer on the  $P-d$  curve obtained in numerical analyses was carried out. The numerical computations were performed on the elastic properties of the material marked as 'B' in Table 2. In the conducted numerical analyses, the parameters of the cohesive layer in  $t-s$  law presented in Table 3 were subject to change.

TABLE 3. Parameters of cohesive zone model  
TABELA 3. Parametry modelu warstwy kohezyjnej

Test symbol	Damage Initiation Stress			Fracture Energy			Penalty Stiffness		
	$t_{tm}$	$t_{ss}$	$t_{tt}$	$G_{Ic}$	$G_{IIc}$	$G_{IIIc}$	$K_{mm}$	$K_{ss}$	$K_{tt}$
	[N/mm <sup>2</sup> ]			[N/mm]			[N/mm <sup>3</sup> ]		
B	100	100	100	3.8	3.8	3.8	10 <sup>5</sup>	10 <sup>5</sup>	10 <sup>5</sup>
I	200	200	200	3.8	3.8	3.8	10 <sup>5</sup>	10 <sup>5</sup>	10 <sup>5</sup>
J	160	160	160	3.8	3.8	3.8	10 <sup>5</sup>	10 <sup>5</sup>	10 <sup>5</sup>
K	50	50	50	3.8	3.8	3.8	10 <sup>5</sup>	10 <sup>5</sup>	10 <sup>5</sup>
L	20	20	20	3.8	3.8	3.8	10 <sup>5</sup>	10 <sup>5</sup>	10 <sup>5</sup>
M	10	10	10	3.8	3.8	3.8	10 <sup>5</sup>	10 <sup>5</sup>	10 <sup>5</sup>
N	5	5	5	3.8	3.8	3.8	10 <sup>5</sup>	10 <sup>5</sup>	10 <sup>5</sup>
S	100	100	100	5.32	5.32	5.32	10 <sup>5</sup>	10 <sup>5</sup>	10 <sup>5</sup>
R	100	100	100	4.56	4.56	4.56	10 <sup>5</sup>	10 <sup>5</sup>	10 <sup>5</sup>
T	100	100	100	3.04	3.04	3.04	10 <sup>5</sup>	10 <sup>5</sup>	10 <sup>5</sup>
U	100	100	100	2.28	2.28	2.28	10 <sup>5</sup>	10 <sup>5</sup>	10 <sup>5</sup>
W	100	100	100	1.52	1.52	1.52	10 <sup>5</sup>	10 <sup>5</sup>	10 <sup>5</sup>
Y	100	100	100	3.8	3.8	3.8	10 <sup>4</sup>	10 <sup>4</sup>	10 <sup>4</sup>
Z	100	100	100	3.8	3.8	3.8	10 <sup>6</sup>	10 <sup>6</sup>	10 <sup>6</sup>

The impact of the  $t_{ss}$  parameter on the  $t$ - $s$  constitutive model shape is illustrated in Figure 7. In accordance with equations (2) and (3), the change in  $t_{ss}$  at constant values of  $K_{ss} = 10^5$  N/mm<sup>3</sup> and  $G_{IIc} = 1$  N/mm results in a changed initiation point  $\delta_{ini}$  and separation point  $\delta_{sep}$  of the cohesive layer in  $t$ - $s$  law.

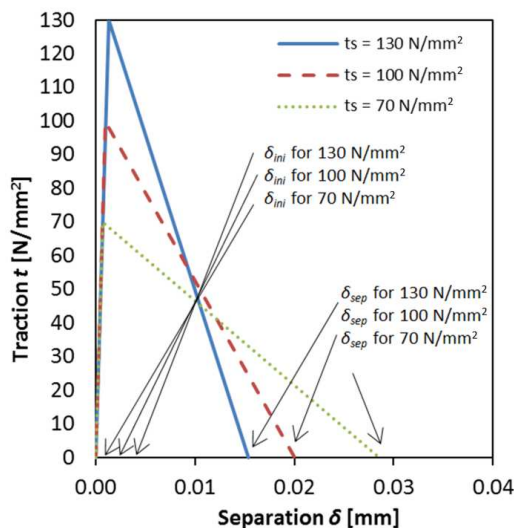


Fig. 7. Impact of  $t_{ss}$  parameter on  $t$ - $s$  constitutive model shape  
Rys. 7. Wpływ parametru  $t_s$  na kształt modelu konstytutywnego  $t$ - $s$

Figure 8 illustrates the  $P$ - $d$  curves obtained in numerical analyses depending on the  $t_{ss}$  parameter of the cohesive layer.

The defined  $t_{ss}$  parameter has a significant impact on the  $P$ - $d$  curve in ENF test modelling. An insufficient  $t_{ss}$  value leads to premature excessive degradation of the cohesive elements. Therefore a smooth shape of the  $P$ - $d$  curve is observed. After an increase in traction stress  $t_{ss}$ , in the range of 50÷150 N/mm<sup>2</sup>, a highly similar laminate response was achieved in comparison with the experimental test. However, an excessive  $t_{ss}$  value (> 160 N/mm<sup>2</sup>) leads to overestimation of beam

strength. Additionally, an improperly selected  $t_{ss}$  parameter leads to unstable growth of crack length (intensive oscillations of force vs. displacement). A similar effect of overestimated strength was described in the study published by Soto et al. [25] who investigated the impact of mesh size on the characteristics of the End Lap Shear test. It is assumed that in the case of improper selection of the number of finite elements in relation to the Cohesive Zone Length ( $\delta_{sep}$ ), the stress distribution on the crack tip vicinity is improper, which leads to incorrect crack initiation and propagation. This effect can result in lack of conformity of the experimental results to the simulations [25]. Liu et al. [7] and Freed and Banks-Sills [26] also concluded that an excessive value of the  $t_{ss}$  parameter can lead to unstable growth of the crack and they recommended using rather a low interface strength.

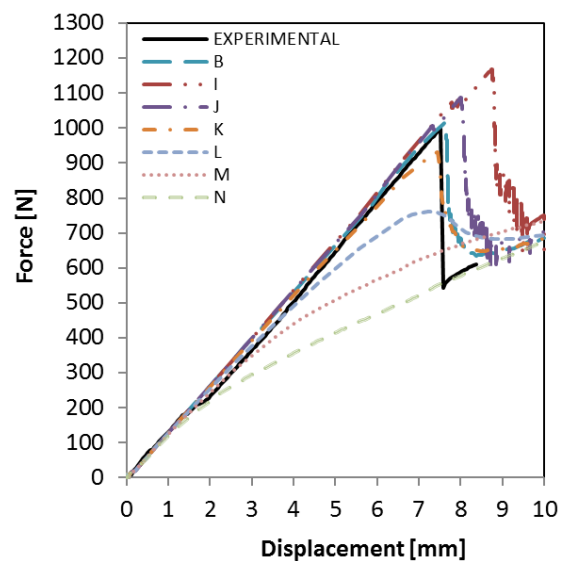


Fig. 8. ENF specimen response depending on adopted  $t_s$  parameter of cohesive layer; markings in accordance with Table 3  
Rys. 8. Odpowiedź próbki ENF w zależności od przyjętego parametru  $t_s$  warstwy kohezyjnej; oznaczenia według tabeli 3

Figure 9 illustrates the shape of the constitutive  $t$ - $s$  model depending on fracture toughness value  $G_{IIc}$  at constant parameters  $t_{ss} = 100 \text{ N/mm}^2$  and  $K_{ss} = 10^5 \text{ N/mm}^3$ . In the case of  $G_{IIc}$  change, initiation point  $\delta_{ini}$  is not subjected to change (as is the case with the  $t_{ss}$  parameter), but only separation point  $\delta_{sep}$  in  $t$ - $s$  law.

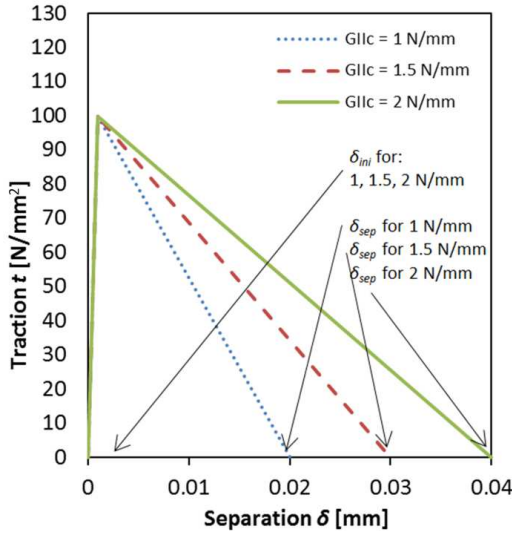


Fig. 9. Impact of fracture toughness  $G_{IIc}$  on  $t$ - $s$  constitutive model shape  
Rys. 9. Wpływ energii pęknięcia  $G_{IIc}$  na kształt modelu konstytutywnego  $t$ - $s$

Figure 10 illustrates the  $P$ - $d$  curves obtained in the numerical analyses of the ENF test depending on crack energy  $G_{IIc}$  in the cohesive layer.

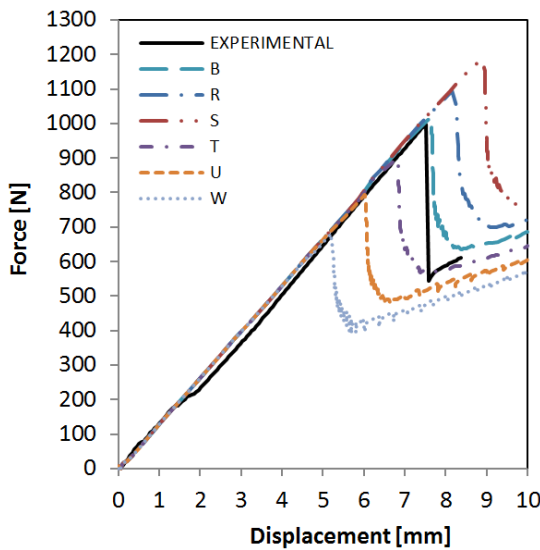


Fig. 10. Response of ENF specimen depending on adopted  $G_{IIc}$  fracture energy of cohesive layer; markings in accordance with Table 3  
Rys. 10. Odpowiedź próbki ENF w zależności od przyjętej energii pęknięcia  $G_{IIc}$  warstwy kohezijnej; oznaczenia według tabeli 3

As in the case of  $t_{ss}$ , fracture toughness  $G_{IIc}$  has a key impact on the response of the composite beam in the ENF test. However, the character of the  $P$ - $d$  curves obtained in the numerical simulations is different. In the case of  $t_{ss}$ , the change in the parameters leads to more ‘sharp’ or ‘flattened’ curves. However, the  $G_{IIc}$  param-

eter has an impact only on the critical point characterized by the energy release and by crack growth. The SERR  $G_{IIc}$  values are determined experimentally for the specified type of material in standardized beam tests, i.e. Interlaminar Fracture Toughness tests for three Fracture Modes. The  $G_{IIc}$  parameter is a material constant and should rather not be changed in order to obtain better conformity of the numerical model to the experimental research.

Figure 11 illustrates the shape of the  $t$ - $s$  constitutive model depending on the  $K_{ss}$  stiffness value of the cohesive layer, at constant parameters, i.e.  $t_{ss} = 100 \text{ N/mm}^2$  and  $G_{IIc} = 1 \text{ N/mm}$ . In the case of  $K_{ss}$  change, initiation point  $\delta_{ini}$  is changed but separation point  $\delta_{sep}$  is constant.

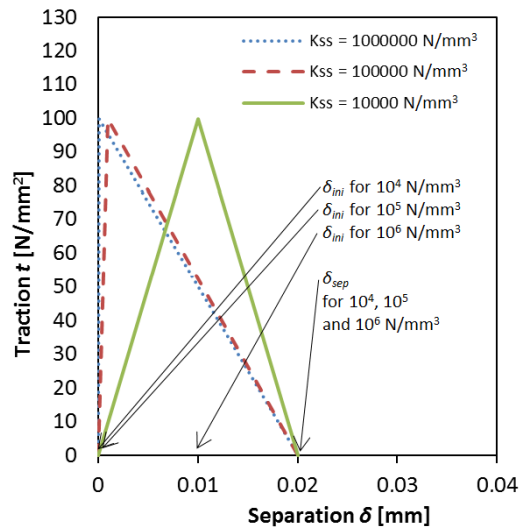


Fig. 11. Impact of  $K_{ss}$  stiffness on  $t$ - $s$  constitutive model shape  
Rys. 11. Wpływ sztywności  $K_{ss}$  na kształt modelu konstytutywnego  $t$ - $s$

Figure 12 illustrates the  $P$ - $d$  curves obtained in numerical analyses of the ENF test depending on the  $K_{ss}$  stiffness value of the cohesive layer.

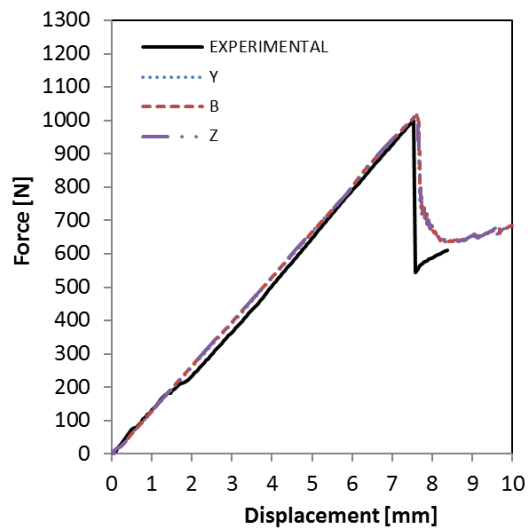


Fig. 12. Response of ENF specimen depending on cohesive layer stiffness  $K_{ss}$ ; markings in accordance with Table 3  
Rys. 12. Odpowiedź próbki ENF w zależności od sztywności  $K_{ss}$  warstwy kohezijnej; oznaczenia według tabeli 3

It can be observed that the  $K_{ss}$  parameter has no impact on the response of the ENF beam. However, in the opinion of Soto [25], the penalty stiffness should be as high as possible in order to avoid the influence of cohesive zone flexibility on global compliance of the structure. In the majority of numerical analyses, the assumed value of the  $K_{ss}$  parameter is equal to about  $10^5 \div 10^6$  N/mm<sup>3</sup>. According to Schellekens and de Borst [27], an excessive value of the  $K_{ss}$  parameter leads to unstable analysis and a very low time increment. This effect extends the numerical computation times significantly. As in the case of the present analyses, Allix et al. [28] also concluded that the  $G_{IIc}$  parameter has a key impact on the mechanical response of cracking laminates modelled by means of CZM. However, it should also be added that the value of the  $t_{ss}$  parameter also has a significant impact on the  $P-d$  curve because its wrong assumption could lead to difficulties obtaining conformity between the  $P-d$  characteristics in the numerical analyses and experimental tests. The composite ENF specimen after the experimental tests as well as after numerical analysis with 'B' parameters (according to Tables 2 and 3) is presented in Figure 13.

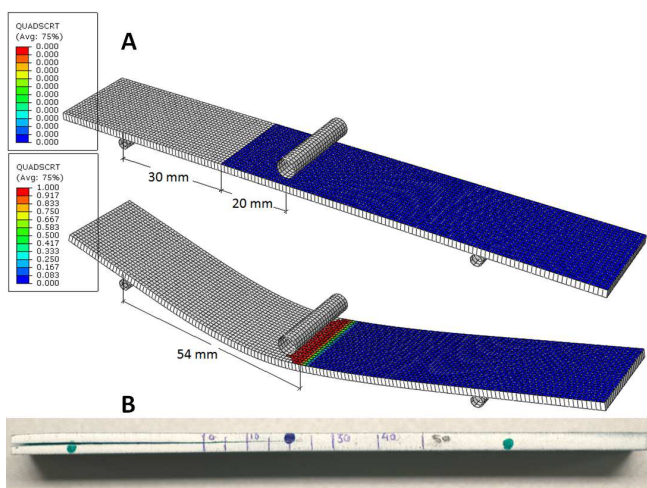


Fig. 13. A) Initial crack length and crack length in composite specimen after ENF test (marked 'B') in numerical analysis; B) Crack length after experimental ENF test

Rys. 13. A) Początkowa długość pęknięcia oraz długość pęknięcia kompozytu po teście ENF (o oznaczeniu 'B'); B) Długość pęknięcia po teście eksperymentalnym

In Figure 13, the failure criterion QUADS for damage initiation of the cohesive layer is shown. A value equal to 1 means that the QUADS criterion is met, according to formula (5). After reaching a value of 1, further degradation of element stiffness occurs and fully degraded cohesive elements are then removing from the analysis. This method simulated the growth of cracks in the researched composite material. The same value of increased crack length was found in both the numerical analysis (about 23÷25 mm) and experimental procedure (about 23÷24 mm). On the basis of Figure 13, which refers to the response of the composite material in respect to global deflection and crack growth produced in

the ENF tests in numerical analysis (marked 'B'), as well as of Figure 10 showing the  $P-d$  curve obtained on the testing machine (marked 'EXPERIMENTAL'), it could be observed that the developed numerical model of unidirectional glass-epoxy composite material with a cohesive layer yields results which are very similar to those obtained during experimental tests.

## CONCLUSIONS

The flexibility of a composite beam subjected to ENF testing in accordance with Euler-Bernoulli beam theory depends on the value of Young's modulus  $E_1$  characterizing composite stiffness along the fibres. Other mechanical parameters describing the elastic behaviour of a fibre composite have no impact on the  $P-d$  curve slope in the initial phase of the Mode II ENF test, based on three point bending. The  $G_{IIc}$  and  $t_{ss}$  parameters have a key impact on the cracking characteristic obtained in the numerical model of the composite material subjected to ENF testing. Defining proper values of the  $t_{ss}$  and  $K_{ss}$  parameters and inputting a  $G_{IIc}$  value determined in additional experimental tests, it is possible to achieve very good agreement of  $P-d$  composite beam response in the numerical analysis and experimental ENF tests. High conformity of the numerical model ('B' marking of  $t-s$  law properties) to the experimental investigations has been achieved in terms of shape, progress and critical values of displacement and force in the ENF test carried out on a GFRP composite. The present study illustrates the impact of  $t-s$  law parameters on the composite beam response in the ENF test. The results of the executed numerical simulations can be used as guidance for defining more advanced and complex numerical models of cracking fibre composites using  $t-s$  law.

## Acknowledgement

*The study has been financed by the Faculty of Mechanical Engineering of Lublin University of Technology in the frame of statutory research works.*

## REFERENCES

- [1] Bieniaś J., Jakubczak P., Surowska B., Dragan K., Low-energy impact behaviour and damage characterization of carbon fibre reinforced polymer and aluminium hybrid laminates, Archives of Civil and Mechanical Engineering 2015, 15(4), 925-932.
- [2] Dadej K., Jakubczak P., Bieniaś J., Surowska B., The influence of impactor energy and geometry on degree of damage of glass fiber reinforced polymer subjected to low-velocity impact, Composites Theory and Practice 2015, 15(3), 163-167.
- [3] Bieniaś J., Jakubczak P., Dadej K., Low-velocity impact resistance of aluminium glass laminates - Experimental and numerical investigation, Composite Structures 2016, 152, 339-348.

- [4] Zhang J., Zhang X., Simulating low-velocity impact induced delamination in composites by a quasi-static load model with surface-based cohesive contact, *Composite Structures* 2015, 125, 51-57.
- [5] Tan W., Brian G.F., Louis N.S.C., Price M., Predicting low velocity impact damage and Compression-After-Impact (CAI) behaviour of composite laminates, *Composites: Part A* 2015, 71, 212-226.
- [6] Jakubczak P., Bienias J., Dadej K., Zawiejski W., The issue of residual strength tests of thin fibre metal laminates, *Composites Theory and Practice* 2014, 14(3) 134-138.
- [7] Liu P.F., Gu Z.P., Peng X.Q., Zheng J.Y., Finite element analysis of the influence of cohesive law parameters on the multiple delamination behaviors of composites under compression, *Composite Structures* 2015, 131, 975-986.
- [8] Dugdale D.S., Yielding of steel sheets containing slit, *Journal of the Mechanics and Physics of Solids* 1960, 8(2), 100-104.
- [9] Barenblatt G.I., The mathematical theory of equilibrium cracks in brittle fracture, *Advances in Applied Mechanics* 1962, 7, 55-129.
- [10] Camanho P.P., Davila C.G., de Moura M.F., Numerical simulation of mixed-mode progressive delamination in the composite materials, *Journal of Composite Materials* 2003, 37(16), 1415-1438.
- [11] Turon A., Camanho P.P., Costaa J., Dávila C.G., A damage model for the simulation of delamination in advanced composites under variable-mode loading, *Mechanics of Materials* 2006, 38(11), 1072-1089.
- [12] Shor O., Vaziri R., Adaptive insertion of cohesive elements for simulation of delamination in laminated composite materials, *Engineering Fracture Mechanics* 2015, 146, 121-138.
- [13] Borg R., Nilsson L., Simonsson K., Simulating DCB, ENF and MMB experiments using shell elements and a cohesive zone model, *Composites Science and Technology* 2004, 64, 269-278.
- [14] Zhao L., Gong Y., Zhang J., Chen Y., Fei B., Simulation of delamination growth in multidirectional laminates under mode I and mixed mode I/II loadings using cohesive elements, *Composite Structures*, 2014, 116, 509-522.
- [15] Lopes C.S., Sadaba S., Gonzalez C., LLorca J., Camanho P.P., Physically-sound simulation of low-velocity impact on fiber reinforced laminates, *International Journal of Impact Engineering* 2015, 1-15.
- [16] Jing-Fen C., Morozov E.V., Krishnakumar S., Simulating progressive failure of composite laminates including in-ply and delamination damage effects, *Composites: Part A*, 2014, 61, 185-200.
- [17] Rots J.G., Strain-softening analysis of concrete fracture specimens. In: Wittmann FH, editor. *Fracture Toughness and Fracture Energy of Concrete*, Elsevier, Amsterdam 1986, 137-148.
- [18] Volokh K.Y., Comparison between cohesive zone models, *Communications in Numerical Methods in Engineering* 2004, 20(11), 845-56.
- [19] Chandra N., Li H., Shet C., Ghonemb H., Some issues in the application of cohesive zone models for metal-ceramic interfaces, *International Journal of Solids and Structures* 2002, 39(10), 2827-2855.
- [20] Bienias J., Gliszczynski A., Jakubczak P., Kubiak T., Majerski K., Influence of autoclaving process parameters on the buckling and postbuckling behaviour of thin-walled channel section beams, *Thin-Walled Structures* 2014, 85, 262-270.
- [21] Budzik M.K., Jumel J., Ben Salem N., Shanahan M.E.R., Instrumented end notched flexure - Crack propagation and process zone monitoring Part II: Data reduction and experimental, *International Journal of Solids and Structures* 2013, 50, 310-319.
- [22] Schon J., Nyman T., Blomb A., Ansell H., Numerical and experimental investigation of a composite ENF-specimen, *Engineering Fracture Mechanics* 2000, 65, 405-433.
- [23] Dassault Systemes Simulia Corp. Abaqus 6.14 Documentation. 2014. Providence, RI, USA.
- [24] Joki R.K., Grytten F., Hayman B., Sørensen B.F., Determination of a cohesive law for delamination modelling - Accounting for variation in crack opening and stress state across the test specimen width, *Composites Science and Technology* 2016, 128, 49-57.
- [25] Soto A., González E.V., Maimí P., Turon A., Sainz de Aja J.R., de la Escalera F.M., Cohesive zone length of orthotropic materials undergoing delamination, *Engineering Fracture Mechanics* 2016, 159, 174-188.
- [26] Freed Y., Banks-Sills L., A new cohesive zone model for mixed mode interface fracture in biomaterials, *Engineering Fracture Mechanics* 2008, 75(15), 4583-4593.
- [27] Schellekens J., de Borst R., A nonlinear finite-element approach for the analysis of mode-i free edge delamination in composites, *International Journal of Solids and Structures* 1993, 30(9), 1239-1253.
- [28] Allix O., Ladeveze P., Corigliano A., Damage analysis of interlaminar fracture specimens, *Composite Structures* 1995, 31, 61-74.